Optimization of Biporous Micropillar Array for Enhanced Heat Transfer Performance

Citation: Wei, Mengyao, Sivanand Somasundaram, Bin He, Qian Liang, Rishi Raj, Chuan Seng Tan, and Evelyn N. Wang. "Optimization of Biporous Micropillar Array for Enhanced Heat Transfer Performance." Volume 8B: Heat Transfer and Thermal Engineering (November 13, 2015). doi:10.1115/imece2015-52651.

As Published: http://dx.doi.org/10.1115/IMECE2015-52651

Publisher: ASME International

Persistent URL: https://hdl.handle.net/1721.1/137101

Version: Final published version: final published article, as it appeared in a journal, conference proceedings, or other formally published context

Proceedings of the ASME 2015 International Mechanical Engineering Congress and Exposition
IMECE2015
November 13-19, 2015, Houston, Texas

IMECE2015-52651

OPTIMIZATION OF BIPOROUS MICROPILLAR ARRAY FOR ENHANCED HEAT TRANSFER PERFORMANCE

Mengyao Wei [1,2]
[1]Singapore-MIT Alliance for Research and Technology (SMART) Centre, Singapore
[2]School of Electrical and Electronics Engineering, Nanyang Technological University, Singapore

Sivanand Somasundaram[1]
[1]Singapore-MIT Alliance for Research and Technology (SMART) Centre, Singapore

Bin He[1]
[1]Singapore-MIT Alliance for Research and Technology (SMART) Centre, Singapore

Qian Liang[1]
[1]Singapore-MIT Alliance for Research and Technology (SMART) Centre, Singapore

Rishi Raj[3]
[3]India Institute of Technology, Patliputra Colony, Bihar 800013, Patna, India

Chuan Seng Tan [1,2]
[1]Singapore-MIT Alliance for Research and Technology (SMART) Centre, Singapore
[2]School of Electrical and Electronics Engineering, Nanyang Technological University, Singapore,
Email: TanCS@ntu.edu.sg

Evelyn N.Wang[1, 4]
[1]Singapore-MIT Alliance for Research and Technology (SMART) Centre, Singapore
[4]Department of Mechanical Engineering, Massachusetts Institute of Technology, Cambridge, United States,
Email: enwang@mit.edu

ABSTRACT

Biporous evaporator wicks for heat pipe and vapor chambers can perform superiorly by reducing the viscous drag with larger pores or channels and simultaneously generate higher capillary pressure with smaller pores radius. Unlike conventional sintered metal biporous wicks, cylindrical silicon micropillar based evaporator with microchannels, possess the following advantages: mature and easily controllable fabrication process, possibility of direct integration with semiconductor devices and no risk of thermal expansion mismatch. In this work, we investigated a biporous wick for the evaporator design, which consists of micro pillar arrays interspersed within micro channels. This design was systematically studied by constructing a mathematical model, by coupling Brinkman's equation with mass and energy conservation equations, to predict the biporous wicks' heat transfer performance. In order to find the best combination of geometric factors that give the highest heat flux at a certain superheat value, optimization in Matlab was done. The effect of diameter to pitch ratio, aspect ratio, channel width and contact angle on wick's permeability, capillary pressure and evaporative heat flux were also investigated. Conclusion was drawn that a higher diameter to pitch ratio of 0.57, reasonable aspect ratio of 1.75~3.22, island to channel width ratio of around 1.96 are preferred in this kind of biporous wick's design. Biporous wick show potential to dissipate heat flux of 515.7 W/cm^2 at superheat of 40 °C, which is 134 % higher compared to monoporous wick.

INTRODUCTION

Miniaturization of size and enhancement in performance of devices on integrated circuits are inevitable drivers for electronics industry and these resulted in high power density and heat flux. Higher operating temperatures may result in accelerated failures and increasingly become a significant factor that limits the performance of electronic components. Phase-change phenomena based thermal management devices, such as heat pipes and vapor chambers have drawn much attention. This is owing to their good capabilities in passively dissipating heat, as well as nearly isothermal characteristics during operation [1]. The limiting component of a heat pipe or vapor chamber's

performance is the evaporator. An effective evaporator should be able to serve the purpose of conducting heat effectively, circulating working fluid with high capillary pressure developed in the porous evaporator wick structure as well as venting vapor efficiently [2, 3]. Capillary limit and boiling limit are the two most significant factors need to be considered when designing evaporator wicks for a vapor chamber. Capillary limit is achieved once the thermal and dynamic balance is disequilibrated and the capillary force developed in the wick is insufficient to cover the pressure loss, which will trigger the occurrence of dryout. On the other hand, once large amount of vapor is being generated without efficient ventilation, vapor blanket will form and the phase change process will be hindered, this is denoted as boiling limit [4, 5]. Conventional wick structures, ranging from grooves, channels, sintered powders to metal mesh, provide limited capillary performance or possess low thermal conductivity only [6-8].

To achieve good vapor venting and liquid supply, biporous wicks with two distinguished pore sizes were explored. This kind of wick structure utilizes large pore as vapor pathway to overcome boiling limit and small pore to provide enough capillary action in liquid circulation and large evaporation area. Previous researches have proven that the adopting of biporous designs can lead to enhancement in effective thermal conductivity, critical heat flux, permeability and capillary pressure of evaporator wicks. Cao et al. [9] examined three biporous Cu wicks fabricated by sintering process and concluded that both heat transfer coefficient and critical heat flux were largely improved for biporous structures compare with monoporous ones. Wang et al. [10] constructed an analytical model to predict the evaporative heat transfer in thin biporous media's thin film, transition and intrinsic regions. They concluded that the biporous structure could lead to increase in evaporating meniscus and has superior performance even with a vapor blanket over the wick surface as the receding of meniscus in big pore will cause the increase of meniscus in small pores due to "sucking effect". With a reduction of pore size, a higher average heat transfer coefficient can be obtained [10]. Semenic et al.[5,11] tested a group of Cu powder sintered biporous wicks with small pore size ranging from 53~63 μm and large pore size of 500~710 μm. With a cluster (μm) to powder (μm) ratio of 600/60 and a thickness of 1mm, a highest heat flux of 494 W/cm^2 can be dissipated at a superheat of 128 °C with a constant heat transfer coefficient of 4.2 W/cm^{2}K. They also found that the optimization of evaporator wicks structures depend on the best combination of parameters including particle size, particle to particle bonding area, cluster diameter, evaporator thickness and radius. Capillary pressure was seen to increase linearly with smaller pore radius while liquid permeability showed the contrary relationship. Vapor permeability was shown to be larger with bigger pore diameter while thermal conductivity of the wick is a function of the small to large pore diameter ratio [12]. For thick Cu sintered biporous wick (2000 and 3000 μm) with large pore size of 455 μm and small pore size of 63 μm, a critical heat flux of 990 W/cm^2 (147°C superheat) can be achieved, which is much larger than the result 300 W/cm^2 (21 °C superheat) of monoporous wicks [2]. Yeh et al. investigated the evaporative heat transfer of sintered Nickel biporous wicks. The evaporator wicks' heat transfer coefficient was found to increase with decreasing particle size and increasing pore former content while sintering temperature does not have much effect on it. Heat transfer coefficient up to 6.4 W/cm^{2}K could be obtained, which is about 6 times higher than monoporous wicks [3]. Li et al.[13], Liu et. al. [14] and Chen et al. [15, 16] also fabricated nickel powder based flat sintered biporous wicks with pore radius of 2.6~53 μm. With methanol as working fluid, the wick can spread heat load from 20~160 W effectively with thermal resistance lies between 0.46 °C /W to 2.28 °C /W. Byon et al. [17] had done research on sintered glass powder biporous wicks with particle size of 40~600 μm and cluster size of 250~1440 μm. A significant enhancement of around 11 times in capillary performance of biporous wicks than monoporous wicks were observed. They also built a semianalytical model and revealed that a cluster size to particle size ratio of 4~6 is preferred for optimal capillary performance [17]. Cai et al [4, 18] developed a carbon nanotube biporous structure for high heat flux applications and investigated the dryout phenomena for pillar-like, stripe-like and zigzag biporous configurations. Heat transport capability of 770 W/cm^2 was demonstrated for stripe-like carbon nanotube biwick structure. Dryout occurred due to fast vapor flow induced liquid splash and was defined as the inflexion point on boiling curve.

The foregoing researches mainly focused on sintered metal biporous wicks. However, it is hard to accurately control the sintering process. Sintered wicks' pore size, roughness and pore interconnectivity is a strong function of sintering temperature and time [12]. Recent 3D microelectronics development also requires efficient direct cooling on hotspots without the introduction of excess thermal interface resistance or thermal expansion mismatch risks [19-21]. Thus evaporator wicks made from Si by micro-electromechanical systems (MEMS) process promises to meet these challenges in terms of its direct integration with semiconductor chips, compatible thermal expansion coefficient with most semiconductors, mature and easily control fabrication process. Although experimental studies have been conducted [22], the geometrical sizes of the biporous wicks were determined on trial-and-error basis without any systematic model as guidance for the optimization of their heat transfer capabilities. In this work, we are investigating a novel evaporator design with cylindrical silicon micropillar arrays to provide capillary force and microchannels serving as local reservoir for micropillar islands. Mathematical model were established to predict the maximum heat flux of the evaporator wicks. Optimization using Matlab were performed to find the optimized combination of wick geometries that give the highest heat flux.

NOMENCLATURE

A	Area (m^2)
K	Permeability (m^2)
L	Half of total wick length (m)
P	Pressure (Pa)
c	Solid fraction
d	Pillar diameter (μm)
h	Pillar height (μm)
l	Pitch (center to center distance) (μm) and width
$q"$	Maximum heat flux (W/cm^2)
rf	Roughness factor of DRIE Si surface $\pi/2$
w	Half microchannel width (μm)
h_{fg}	Latent heat (J/kg)
k	Thermal conductivity$(W/m\bullet K)$
u	Liquid velocity (m/s)
θ	Contact angle of water on Si surface (°)
ε	Porosity
σ	Surface tension of water(N/m)
μ	Viscosity of water$(Pa\bullet s)$
ρ_l	Density (kg/m^3)
ΔE	Decrease in surface energy as liquid fills one unit cell
ΔT	Superheat $(°C)$
ΔV	Volume of liquid filling one cell

SUBSCRIPT

m	Meniscus area
p	Projected meniscus
fg	Latent heat
$2D$	Planar
$3D$	Array of pillars
eff	Effective
i	Island
cap	Capillary
la	Drop along the channel
in	Inlet
$mean$	Mean

ANALYTICAL MODEL

A microengineered silicon surface with deep reactive ion etched (DRIE) cylindrical silicon pillars and micro-channels is shown in Fig. 1. The microchannels serve as liquid reservoir for enhanced heat transfer performance. In the current model the liquid supply is only from two sides as shown in the Fig .1 and liquid meniscus was assumed to be pinned by the pillar top. Dryout regime was not reached in this model. Analytical model will be deduced based on evaporation phenomena only as follows.

For cylindrical silicon micro-pillar surface, the capillary pressure was determined by Xiao et al. [23] based on interfacial energy minimization and is defined as change in surface free energy per unit volume:

$$P_{cap}=\frac{\Delta E}{\Delta V}=\frac{\sigma rf\cos\theta\pi dh+\sigma\cos\theta A_p-\sigma A_m}{\Delta V} \quad (1)$$

where $A_p=l^2-\frac{1}{4}\pi d^2$ is the projected meniscus area.

Volume of the liquid ΔV and area of menisci A_m are correlated to micropillar geometric parameters by fitting the results in Surface Evolver simulation and are expressed as:

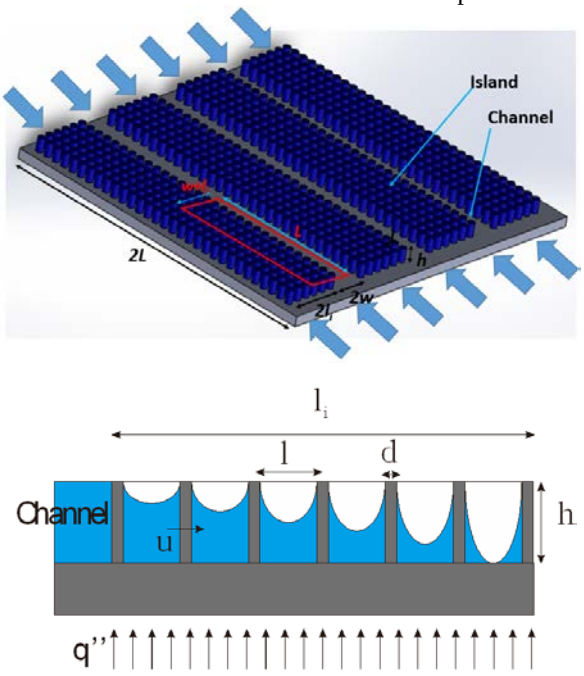

Figure 1: BIPOROUS EVAPORATOR WICK OF CYLINDRICAL SILICON MICROPILLAR ISLANDS WITH MICROCHANNELS

$$\frac{hA_p-\Delta V}{A_p(l-d)}=-0.175-0.345rf\cos\theta+4.07(\frac{d}{l})+0.924(rf\cos\theta)^2 \quad (2)$$
$$-5.83(rf\cos\theta)(\frac{d}{l})-2.80(\frac{d}{l})^2-0.439(rf\cos\theta)^3+2.41(rf\cos\theta)^2(\frac{d}{l})$$
$$+2.71(rf\cos\theta)(\frac{d}{l})$$

$$\frac{A_m}{A_p}=0.43+0.73rf\cos\theta+3.76(\frac{d}{l})-0.046(rf\cos\theta)^2-5.53(rf\cos\theta)(\frac{d}{l}) \quad (3)$$
$$-4.05(\frac{d}{l})^2-0.124(rf\cos\theta)^3+1.77(rf\cos\theta)^2(\frac{d}{l})+4.66(rf\cos\theta)(\frac{d}{l})^2$$

By substituting Eq. (2) and (3) into (1), capillary pressure of the wick as a function of pillar dimensions can be obtained. The above model is valid for $d/l<0.57$ and $h/l>1$[23].

Permeability of planar pillar arrays with flat meniscus has been studied by Sangani et al. [24] and is expressed as:

$$K_{2D} = l^2 \frac{\ln c^{-1/2} - 0.738 + c - 0.887c^2 + 2.038c^3 + o(c4)}{4\pi} \quad (4)$$

Where c is the solid fraction of the wick structure and

$$c = \frac{\pi d^2}{4l^2} \quad (5)$$

Later Byon et al. [25] refined the permeability model of micropillar arrays by considering the effect of liquid meniscus shape in conjunction with Darcy's law. They expressed the permeability of cylindrical micropillar wick structure as:

$$K = A_1 A_2 K_{3D,flat} \quad (6)$$

$$K_{3D,flat} = K_{2D}\left[1 - \frac{\exp(2\sqrt{\frac{\varepsilon}{K_{2D}}}h_{eff}) - 1}{\sqrt{\frac{\varepsilon}{K_{2D}}}h_{eff}(\exp(2\sqrt{\frac{\varepsilon}{K_{2D}}}h_{eff}) + 1)}\right] \quad (7)$$

where

$$h_{eff} = h - d\Delta h \quad (8)$$

$$\Delta h = 0.01476 + 0.85009\cos\theta + 0.215\frac{d}{l} + 0.18979(\cos\theta)^2 - 3.46929(\frac{d}{l})(\cos\theta) \quad (9)$$
$$-0.28868(\frac{d}{l})^2 + 1.05357(\frac{d}{l})(\cos\theta)^2 + 3.12583(\cos\theta)(\frac{d}{l})^2 - 1.4243(\frac{d}{l})^2(\cos\theta)^2$$

A_1 and A_2 are parameters included to account for the change of wetted area and cross-sectional area respectively, they are expressed as:

$$A_1 = \frac{h_{eff} + \frac{\varepsilon d}{4(1-\varepsilon)}}{h + \frac{\varepsilon d}{4(1-\varepsilon)}} \quad \text{and} \quad A_2 = \frac{h_{eff}}{h} \quad (10)$$

By substituting Eq. (4),(7),(8),(9) and (10)into(6),permeability of cylindrical micropillar wicks can be obtained.

Qian et al. [21] have predicted the evaporative heat flux for uniform micropillar array wicks using Brinkman equation as:

$$q'' = \frac{2P_{cap}\rho_l h_{fg} hK}{\mu L^2}\left[1 - \frac{\tanh(\sqrt{\frac{\varepsilon}{K}}h)}{\sqrt{\frac{\varepsilon}{K}}h}\right] \quad (11)$$

For the new design in Fig. 1 with island structures with width $2l_i$ consist of silicon micropillars and microchannel with channel width of $2w$, the following assumptions are made:

(a) Meniscus in microchannel is ignored

(b) Heat transfer occurs in pillared area only, since the thin film evaporation areas in the island is much larger than that in the channel

(c) $l_i \geq 10\,l$

Based on Eq. (11) and taking l_i as characteristic length, with the assumption of no heat transfer inside microchannel, evaporative heat flux in channel biporous wicks can be expressed as:

$$q'' = \frac{l_i}{l_i + w}\frac{2\Delta P\rho_l h_{fg} hK}{\mu l_i^2}\left[1 - \frac{\tanh(\sqrt{\frac{\varepsilon}{K}}h)}{\sqrt{\frac{\varepsilon}{K}}h}\right] \quad (12)$$
$$= \frac{l_i}{l_i + w}\frac{2(P_{cap} - P_{la})\rho_l h_{fg} hK}{\mu l_i^2}\left[1 - \frac{\tanh(\sqrt{\frac{\varepsilon}{K}}h)}{\sqrt{\frac{\varepsilon}{K}}h}\right]$$

where P_{la} is the pressure drop in microchannel. Liquid transport inside microchannel is governed by Navier-Stokes equation:

$$\rho_l u \cdot \nabla u = \mu\nabla^2 u - \nabla P \quad (13)$$

and continuity equation:

$$\nabla \cdot u = 0 \quad (14)$$

By scaling analysis, the mean flow velocity at channel inlet can be expressed as:

$$u_{in} = -\frac{l_i^2}{\mu}\frac{P_{la}}{L} f(\frac{w}{l_i}, \frac{h}{l_i}) \quad (15)$$

where $f(\frac{w}{l_i}, \frac{h}{l_i})$ is a geometric dependent coefficient and is a function of channel width l_i, island width w and channel height h. Flow transport inside microchannels was simulated with COMSOL 4.3 to obtain the function $f(\frac{w}{l_i}, \frac{h}{l_i})$ by curve fitting of numerical results.

The following boundary conditions were applied in COMSOL , as shown in Fig.2:

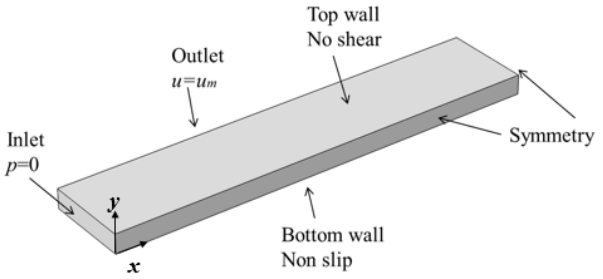

Figure 2: BOUNDARY CONDITIONS APPLIED FOR FLOW INSIDE MICROCHANNEL SIMULATION WITH COMSOL 4.3

(a) No slip condition at bottom: $u|_{y=0} = 0$

(b) Shear free at top: $\frac{\partial u}{\partial y}|_{y=h} = 0$

(c) Symmetric boundary conditions at sidewall

(d) Inlet $P|_{x=0} = 0$

(e) Outlet $u|_{z=w} = u_{mean}$

The expression for $f(\frac{w}{l_i}, \frac{h}{l_i})$ was obtained to be:

$$f(\frac{w}{l_i},\frac{h}{l_i}) = [-2.3868\times10^{-4} + 4.8541\times10^{-2}\frac{h}{l_i} - 1.4325(\frac{h}{l_i})^2]\times\exp(-\frac{\frac{w}{l_i}}{0.11073 - 0.23438\frac{h}{l_i} + 4.57228(\frac{h}{l_i})^2}) + [-1.3911\times10^{-4} + 7.1494\times10^{-3}\frac{h}{l_i} + 0.8331(\frac{h}{l_i})^2] \quad (16)$$

Pressure drop along the microchannel will be:

$$P_{la} = \frac{q"L^2}{whf(\frac{w}{l_i},\frac{h}{l_i})}\frac{\mu}{\rho_l h_{fg} l_i} \quad (17)$$

By substituting Eq. (16) and (17) into (12), the evaporative heat flux for microchannel based biporous structures can be calculated using the following equation:

$$q" = \frac{\frac{2\rho_l h_{fg} hK}{l_i\mu}\left[1 - \frac{\tanh(\sqrt{\frac{\varepsilon}{K}}h)}{\sqrt{\frac{\varepsilon}{K}}h}\right]\frac{1}{l_i + w}P_{cap}}{1 + \frac{2hK}{l_i^2}\left[1 - \frac{\tanh(\sqrt{\frac{\varepsilon}{K}}h)}{\sqrt{\frac{\varepsilon}{K}}h}\right]\frac{1}{l_i + w}\frac{L^2}{whf(\frac{w}{l_i},\frac{h}{l_i})}} \quad (18)$$

OPTIMIZATION

By plotting heat flux (*q"*) versus channel width (*w*), the following curve can be obtained, as shown in Fig. 3. Range of *w* was taken to be 10 to 2000 μm while *d*, *h*, *l*, l_i, *L* used for calculations were 3 μm, 6 μm, 6 μm, 200 μm and 5mm respectively.

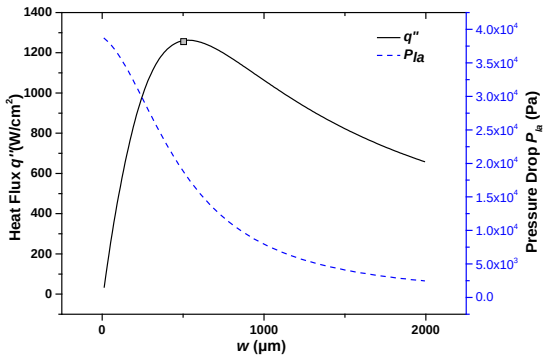

Figure 3: HEAT FLUX AND PRESSURE DROP VARIATION WITH MICROCHANNEL WIDTH

It can be observed that, as microchannel becomes wider, pressure drop decreases so the heat flux dissipated increases with increase in channel width due to higher absolute capillary pressure. But beyond a critical point the loss in actual heat transfer area is so high and heat flux starts decreasing. Thus there exist a maximum value of *w* for a certain combination of other geometric factors. Therefore optimization need to be done in Matlab R2013a to find the optimal combination of geometric parameters (d, h, l, l_i, w) that gives the highest evaporative heat flux. An inbuilt optimization tool '*fmincon*' was used. At a certain wall superheat boiling is initiated, which is not desirable for stable cooling mechanism inside a heat pipe or vapor chamber. However, this critical superheat value depends on a lot of factors, such as fluid thermodynamic properties and surface properties. So the optimized results are presented as a function of maximum allowable superheat and superheat values were limited in the range of 1 °C to 40 °C based on the allowable working temperature for electronic devices. Final value for superheat will be determined experimentally in future work. Thermodynamic properties of water (μ, ρ_l, h_{fg}, σ) at different temperature values were adopted [26]. Constraints used for optimization of Eq. (18) were:

(a) $d / l < 0.57$
(b) $h / l > 1$
(c) $l_i \geq 10l$
(d) $q"\frac{l_i + w}{l_i} = k_{eff}\frac{\Delta T}{h}$

where ΔT is the superheat and k_{eff} is the effective thermal conductivity of the silicon micropillar island and is geometric dependent. Expression of k_{eff} was obtained by numerical simulation of a unit cell of micropillar and water in COMSOL 4.3. Boundary conditions applied for obtaining effective thermal conductivity were constant heat flux at bottom of unit cell, symmetric condition at sidewalls and natural convection at unit cell top. Parameters like pillar diameter and pitch were varied to obtain corresponding effective thermal conductivity values of the cell and the relationship between k_{eff}, *d* and *l* was curve fitted to obtain the equation and its expression is

$$k_{eff} = 6.02633(\frac{d}{l})^2 - 3.19508\frac{d}{l} + 2.12324 \quad (19)$$

Lower bound (*lb*) and upper bound (*ub*) for geometric sizes *d*, *h*, *l*, l_i, *w*, were set to be *lb*=[3,6, 6, 10, 10] and *ub*=[100, 100, 100, 500, 2000] with a unit of μm.

RESULTS

Optimized Geometries

Matlab optimization in Fig. 4. As shown in Fig. 4(a) and 4(b), for each allowable maximum superheat value, there is a best combination of geometric sizes for pillar and channel. At higher heat flux, pillar with larger sizes are preferred. With increasing superheat of up to 40 °C, a very high evaporative heat flux of around 515.7 W/cm^2 can be achieved with *d*=3.42 μm, *h*=11.02 μm, *l*=6 μm, l_i= 98.2 μm, *w*= 58.03 μm and *L*= 5mm. Such a high heat dissipation ability of biporous wick is owing to high capillary pressure and large thin film evaporation area provided by pillared islands. The existence of microchannel can reduce the effective liquid propagation length and viscous resistance for liquid transportation. Thus it can

ensure sufficient liquid supply for the wick while preventing dryout from occurring. Due to the aforementioned reasons, biporous wicks have the potential to spread high heat flux effectively with reasonable superheat.

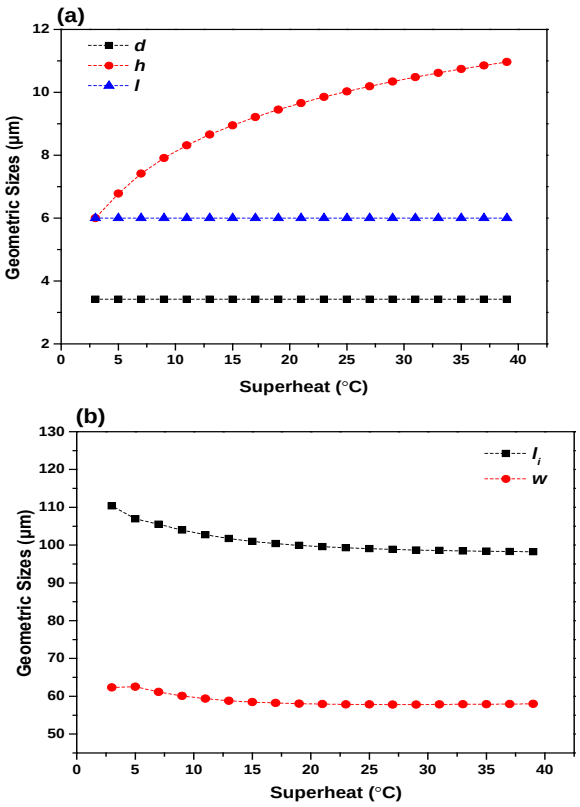

Figure 4: OPTIMIZATION RESULTS (a) OPTIMIZED GEOMETRIC SIZES (*d* :DIAMETER, *h* :HEIGHT, *l* :PITCH) (b) OPTIMIZED ISLAND WIDTH (l_i) AND CHANNEL WIDTH(*w*) AT A CERTAIN SUPERHEAT VALUE

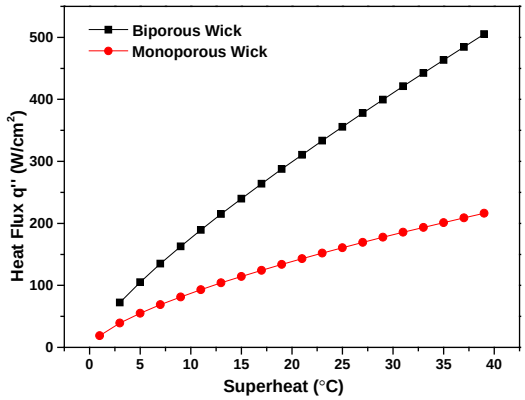

Figure 5: MAXIMUM ACHIEVABLE HEAT FLUX AT EACH ALLOWABLE SUPERHEAT VALUE FOR MONOPOROUS AND BIPOROUS WICKS

Comparison of performance of biporous and monoporous wicks with the same wick size of L=5 mm and contact angle of 10° is illustrated in Fig. 5 with maximum achievable heat flux at a certain superheat value plotted. From Fig. 5, it can be concluded that with the adoption of biporous wicks can significantly enhance the wick's performance. At a superheat of 40 °C, maximum heat flux of monoporous wick is 220 W/cm^2 while that of biporous wick is 515.7 W/cm^2, which corresponds to 134 % enhancement in the performance.

Geometric Effects

Optimization results at superheat of 25°C is adopted as reference to study the effect of geometric parameters of pillars, channel width and contact angle's influence on performance of biporous wicks. Optimized combination of these factors at 25°C superheat is: d=3.42 μm, h= 10.02 μm, l=6 μm, l_i=99.04 μm, w=59.03 μm with wick length L of 5 mm for contact angle of 10°, which correspond a heat flux of 355.7 W/cm^2.

The effect of d/l ratio on heat transport capability of biporous wick by keeping constant d and tuning l is shown in Fig. 6(a). l is limited in the range such that d/l<0.57 and h/l>1 The trends reveals that a higher d/l ratio will result in larger capillary pressure, smaller permeability and higher heat flux. The higher heat flux is mainly attributed to the better capillary performance developed, more thin film evaporation areas in pillar with larger d/l ratio as well as higher effective thermal conductivity according to Eq. (19).

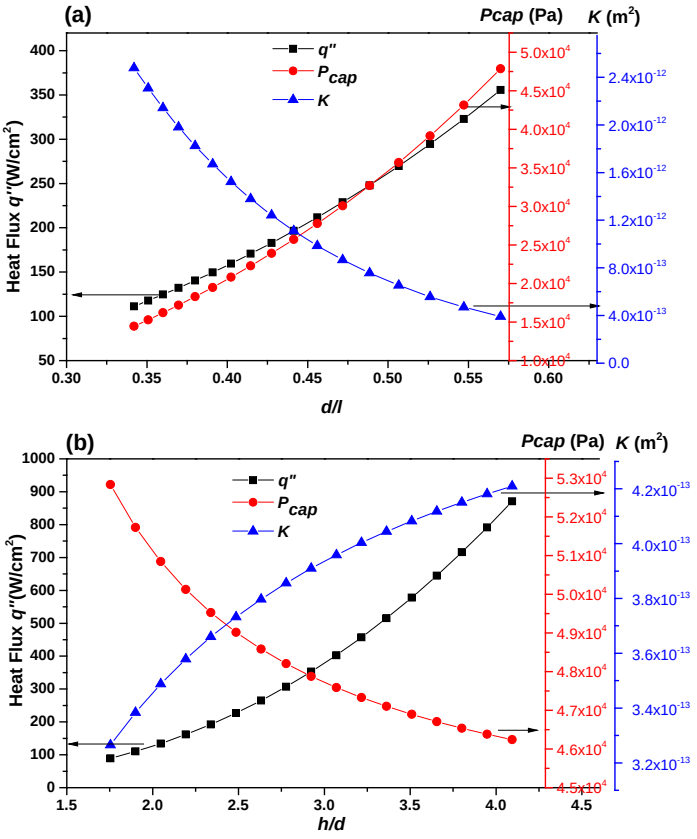

Figure 6: EFFECT OF (a) d/l (b) h/d RATIO ON CAPILLARY PRESSURE *Pcap*, PERMEABILITY *K* AND HEAT FLUX q" OF BIPOROUS EVAPORATOR WICK WITH CONSTANT ISLAND AND CHANNEL SIZES

Effect of *h/d* ratio on biporous wicks' performance is shown in Fig. 6(b). By observing the result, we can conclude that pillars with larger aspect ratios are preferred for high heat flux applications. This is because viscous force exerted by the substrate will be less dominant for pillars with taller height. Volumetric flow rate will also increase with an increasing height of pillars. Thus with higher pillar height, permeability of the pillared area will increase, which is in agreement with results from the literature [27, 28]. However, the pillar cannot be infinitely long as large thermal resistance and superheat will be induced with tall pillars, according to the expression that $\Delta T = q'' h / k_{eff}$. Moreover, fabrication of pillars with large aspect ratio will be rather difficult, which also limits the choice of pillar height [29].

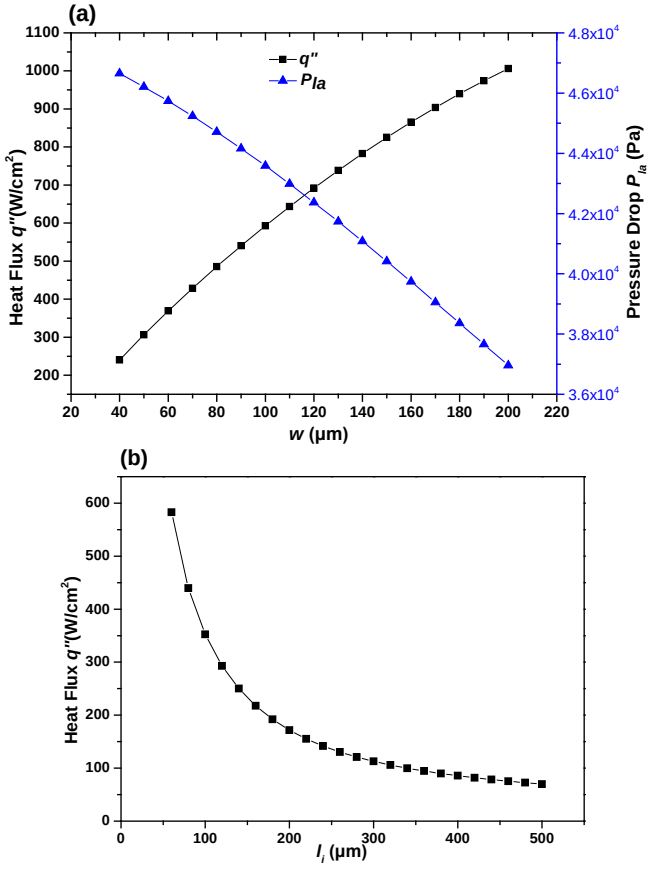

Figure 7: EFFECT OF (a) CHANNEL WIDTH *w* (b) ISLAND WIDTH l_i ON BIPOROUS EVAPORATOR WICK WITH CONSTANT PILLAR GEOMETRIES

Based on Fig. 4(b), we found that optimized island size approaches 98 μm and optimized channel size is around 58 μm. In order to limit the superheat into a reasonable range, microchannel was compromised to have a smaller optimized value than the value shown in Fig. 3. Thus the graph in Fig. 7(a) only covers the left portion of the w versus *q"* plot in Fig. (3).Therefore Fig. 7(a) has shown that a wider microchannel is preferred to dissipate higher heat flux. This is attributed to lower pressure drop in a wider channel. Island with smaller width can result in better heat transfer performance as shown in Fig. 7(b), as there is reduction in propagation length for liquid. However smaller islands would mean lower effective heat transfer area, which would lead to very high wall superheat value. Therefore, to satisfy the all the constraints the optimal value was 98 μm.

Contact angle is found to have significant effect on biporous wick's heat transfer capabilities, as shown in Fig. 8. The effect of varying contact angle from 10° to 38° is shown. A smaller contact angle, which is an indication of good hydrophilicity, is desired for better heat spreading of the wick. This can be achieved by surface modification, surface cleaning and plasma treatment.

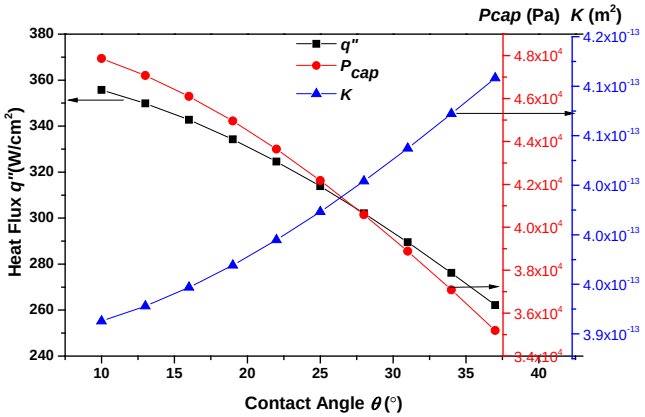

Figure 8: EFFECT OF CONTACT ANGLE ON CAPILLARY PRESSURE *Pcap*, PERMEABILITY *K* AND HEAT FLUX *q"* OF BIPOROUS EVAPORATOR WICK

CONCLUSIONS

A novel design of cylindrical silicon micropillar based islands with microchannel biporous wick structures were proposed for advanced thermal management by vapor chamber. Mathematical model to predict the evaporative heat transfer performance of this biporous wick was constructed. Optimization in Matlab was carried out to find the best combination of geometric factors for biporous wicks. The dependence of capillary pressure, permeability and heat flux on pillars' diameter, height, pitch, channel width, island width and contact angle were also investigated. It was found that a higher *d/l* ratio of 0.57, moderate aspect ratio of 1.75~3.22, microchannel width of 58 μm, pillar island size of 98 μm and smaller contact angle are preferred in order to dissipate high heat flux effectively. This biporous wick with channel design was proven to have much superior performance as it can have up to 2.34 times higher heat transfer capability compared to monoporous wicks. This paper can serve as reference and guidance for the design of biporous wicks. Experimental validation of the model is planned to be carried out in the future study.

ACKNOWLEDGMENTS

This research was supported by the National Research Foundaiton Singapore through Singapore MIT Alliance for Research and Technology's Low Energy Electronic Systems (LEES) IRG.

REFERENCES

[1] M. Zaghdoudi, S. Maalej, J. Mansouri, and M. Sassi, "Flat miniature heat pipes for electronics cooling: State of the art, experimental and theoretical analysis," International Journal of Engineering and Applied Sciences, vol. 7, pp. 166-189, 2011.

[2] T. Semenic and I. Catton, "Experimental study of biporous wicks for high heat flux applications," International Journal of Heat and Mass Transfer, vol. 52, pp. 5113-5121, 2009.

[3] C.C. Yeh, C.N. Chen, and Y.M. Chen, "Heat transfer analysis of a loop heat pipe with biporous wicks," International Journal of Heat and Mass Transfer, vol. 52, pp. 4426-4434, 2009.

[4] Q. Cai and Y.C. Chen, "Investigations of biporous wick structure dryout," Journal of Heat Transfer, vol. 134, p. 021503, 2012.

[5] T. Semenic, Y.Y. Lin, and I. Catton, "Biporous sintered copper for closed loop heat pipe evaporator," in ASME 2005 International Mechanical Engineering Congress and Exposition, 2005, pp. 21-25.

[6] R. Ranjan, J. Y. Murthy, and S. V. Garimella, "Analysis of the wicking and thin-film evaporation characteristics of microstructures," Journal of Heat Transfer, vol. 131, p. 101001, 2009.

[7] R. Ranjan, A. Patel, S. V. Garimella, and J. Y. Murthy, "Wicking and thermal characteristics of micropillared structures for use in passive heat spreaders," International Journal of Heat and Mass Transfer, vol. 55, pp. 586-596, 2012.

[8] J. A. Weibel, S. V. Garimella, and M. T. North, "Characterization of evaporation and boiling from sintered powder wicks fed by capillary action," International Journal of Heat and Mass Transfer, vol. 53, pp. 4204-4215, 2010.

[9] X. Cao, P. Cheng, and T. Zhao, "Experimental study of evaporative heat transfer in sintered copper bidispersed wick structures," Journal of thermophysics and heat transfer, vol. 16, pp. 547-552, 2002.

[10] J. Wang and I. Catton, "Evaporation heat transfer in thin biporous media," Heat and mass transfer, vol. 37, pp. 275-281, 2001.

[11] T. Semenic, Y. Y. Lin, I. Catton, and D. B. Sarraf, "Use of biporous wicks to remove high heat fluxes," Applied Thermal Engineering, vol. 28, pp. 278-283, 2008.

[12] T. Semenic, Y.-Y. Lin, and I. Catton, "Thermophysical properties of biporous heat pipe evaporators," Journal of Heat Transfer, vol. 130, p. 022602, 2008.

[13] H. Li, Z. Liu, B. Chen, W. Liu, C. Li, and J. Yang, "Development of biporous wicks for flat-plate loop heat pipe," Experimental Thermal and Fluid Science, vol. 37, pp. 91-97, 2012.

[14] Z. Liu, H. Li, B. Chen, J. Yang, and W. Liu, "Operational characteristics of flat type loop heat pipe with biporous wick," International Journal of Thermal Sciences, vol. 58, pp. 180-185, 2012.

[15] B. Chen, W. Liu, Z. Liu, H. Li, and J. Yang, "Experimental investigation of loop heat pipe with flat evaporator using biporous wick," Applied Thermal Engineering, vol. 42, pp. 34-40, 2012.

[16] B. Chen, Z. Liu, W. Liu, J. Yang, H. Li, and D. Wang, "Operational characteristics of two biporous wicks used in loop heat pipe with flat evaporator," International Journal of Heat and Mass Transfer, vol. 55, pp. 2204-2207, 2012.

[17] C. Byon and S. J. Kim, "Capillary performance of bi-porous sintered metal wicks," International Journal of Heat and Mass Transfer, vol. 55, pp. 4096-4103, 2012.

[18] Q. Cai and C.-L. Chen, "Design and test of carbon nanotube biwick structure for high-heat-flux phase change heat transfer," Journal of Heat Transfer, vol. 132, p. 052403, 2010.

[19] Q. Cai, B.-c. Chen, and C. Tsai, "Design, development and tests of high-performance silicon vapor chamber," Journal of Micromechanics and Microengineering, vol. 22, p. 035009, 2012.

[20] C. Gillot, A. Laï, M. Ivanova, Y. Avenas, C. Schaeffer, and E. Fournier, "Experimental study of a flat silicon heat pipe with microcapillary grooves," in InterSociety Conference on Thermal and Thermomechanical Phenomena in Electronic Systems, 2004.

[21] L. Qian, R. Raj, S. Adera, S. Somasundaram, C.S. Tan, and E. N. Wang, "Experiment and modeling of microstructured capillary wicks for thermal management of electronics," in Electronics Packaging Technology Conference (EPTC 2013), 2013 IEEE 15th, 2013, pp. 592-597.

[22] D. Ćoso, V. Srinivasan, M.-C. Lu, J.-Y. Chang, and A. Majumdar, "Enhanced heat transfer in biporous wicks in the thin liquid film evaporation and boiling regimes," Journal of Heat Transfer, vol. 134, p. 101501, 2012.

[23]R. Xiao, R. Enright, and E. N. Wang, "Prediction and optimization of liquid propagation in micropillar arrays," Langmuir, vol. 26, pp. 15070-15075, 2010.

[24] A. Sangani and A. Acrivos, "Slow flow past periodic arrays of cylinders with application to heat transfer," International journal of Multiphase flow, vol. 8, pp. 193-206, 1982.

[25] C. Byon and S. J. Kim, "The effect of meniscus on the permeability of micro-post arrays," Journal of Micromechanics and Microengineering, vol. 21, p. 115011, 2011.

[26] D.-Y. Peng and D. B. Robinson, "A new two-constant equation of state," Industrial & Engineering Chemistry Fundamentals, vol. 15, pp. 59-64, 1976.

[27] C. Byon and S. J. Kim, "Study on the capillary performance of micro-post wicks with non-homogeneous configurations," International Journal of Heat and Mass Transfer, vol. 68, pp. 415-421, 2014.

[28] Y. Nam, S. Sharratt, C. Byon, S. J. Kim, and Y. S. Ju, "Fabrication and characterization of the capillary performance of superhydrophilic Cu micropost arrays," Microelectromechanical Systems, Journal of, vol. 19, pp. 581-588, 2010.

[29] M. Wei, S. Somasundaram, B. He, Q. Liang, C. S. Tan, and E. N. Wang, "Experimental characterization of Si micropillar based evaporator for advanced vapor chambers," in Electronics Packaging Technology Conference (EPTC), 2014 IEEE 16th, 2014, pp. 335-34